

# hsa\_circ\_0010889 downregulation inhibits malignant glioma progression by modulating the miR-590-5p/SATB1 axis

Zhi Wu<sup>1</sup>, Quanlin Guan<sup>2</sup>

<sup>1</sup>Department of Neurosurgery, The First Hospital of Lanzhou University, Lanzhou, Gansu 730000, China

<sup>2</sup>Department of Oncological Surgery, The First Hospital of Lanzhou University, Lanzhou, Gansu 730000, China

**Correspondence to:** Quanlin Guan; **email:** [guanql@lzu.edu.cn](mailto:guanql@lzu.edu.cn)

**Keywords:** glioma, hsa\_circ\_0010889, miR-590-5p, SATB1, malignant progression

**Received:** April 10, 2023

**Accepted:** July 6, 2023

**Published:** August 3, 2023

**Copyright:** © 2023 Wu and Guan. This is an open access article distributed under the terms of the [Creative Commons Attribution License](https://creativecommons.org/licenses/by/3.0/) (CC BY 3.0), which permits unrestricted use, distribution, and reproduction in any medium, provided the original author and source are credited.

## ABSTRACT

Glioma is a general neurological tumor and circular RNAs (circRNAs) have been implicated in glioma development. However, the underlying mechanisms and circRNA biological functions responsible for the regulation of glioma progression remain unknown. In this study, we employ next-generation sequencing (NGS) to investigate altered circRNA expression in glioma tissues. Regulatory mechanisms were studied using luciferase reporter analyses, transwell migration, CCK8, and EdU analysis. Tumorigenesis and metastasis assays were utilized to determine the function of hsa\_circ\_0010889 in glioma. Our results showed that hsa\_circ\_0010889 expression increased in glioma cell lines and tissues, indicating that hsa\_circ\_0010889 may be involved in glioma progression. Downregulation of hsa\_circ\_0010889 inhibited glioma invasion and proliferation in both *in vitro* and *in vivo* experiments and luciferase report assays found that miR-590-5p and SATB1 were downstream targets for hsa\_circ\_0010889. SATB1 overexpression or miR-590-5p inhibition reversed glioma cells proliferation and migration post-silencing of hsa\_circ\_0010889. Taken together, our study demonstrates that hsa\_circ\_0010889 downregulation inhibits glioma progression through the miR-590-5p/SATB1 axis.

## INTRODUCTION

Glioma is a major primary brain tumor, resulting in ~75% of malignant central nervous system (CNS) cancers among adults [1, 2]. Currently, resection surgery and temozolomide (TMZ)-based chemotherapy and radiotherapy are the main treatment methods for glioma. Nevertheless, multidrug resistance, recurrence, and metastasis are often important factors associated with poor clinical efficacy. Therefore, glioma remains an incurable malignancy with a mean survival duration of around 12–15 months [3, 4]. Therefore, it is essential to identify unknown pathogenic mechanisms associated with glioma progression and to identify diagnostic markers and precise therapeutic targets.

Circular RNAs (circRNAs) is a type of single-stranded noncoding RNA having covalently closed-loop structures,

which are considered as promising biomarkers and targets for the diagnosis and treatment of many diseases, particularly cancer. Accumulating evidence suggests that EWSR1-induced circNEIL3/IGF2BP3 enhances glioma progression by regulating macrophage polarization [5] and circRNA-0002109 enhances glioma malignant progresses by regulating the miR-129-5P/EMP2 axis [6]. Exosomal circRNA\_104948 promotes glioma progression via the regulation of miR-29b-3p/DNMT3B/MTSS1 signaling [7]. However, the role of circRNA in glioma progression remains largely unclear.

The present study found that hsa\_circ\_0010889 expression increased in glioma cell lines and tissues. Downregulation of hsa\_circ\_0010889 inhibited glioma progression in both *in vitro* and *in vivo* experiments. Luciferase reporter assay results showed that miR-590-5p and SATB1 were downstream targets for hsa\_circ

0010889. The aim of the present study was to discuss the regulation mechanism of hsa\_circ\_0010889 in glioma.

## MATERIALS AND METHODS

### Animal use and ethical statement

Nude BALB/c female mice (four weeks old, 15–20 g) were obtained from SLAC Laboratory Animal Co. Ltd., Shanghai, China. They were housed in independently ventilated cages and kept at 24–26°C, with constant humidity and a 12-h light/dark cycle. The Ethics Committee of The First Hospital of Lanzhou University oversaw all the procedures (LDYYLL2021-23).

### RNA sequencing, quantification, and identification of circRNAs

Total RNA was extracted from pairs of freshly frozen glioma and adjacent tissues. An Agilent 2200 system (Agilent Technologies, Santa Clara, CA, USA) was used to confirm the RNA quality. The RiboMinus eukaryote kit (Qiagen, Valencia, CA, USA) was used to remove ribosomal RNA followed by cDNA library construction. NGS was carried out using the Illumina HiSeq 3000 (Illumina, San Diego, CA, USA) and the reads were aligned to the GRCH37.p13 reference. Unmapped reads were collected to characterize circRNAs. The reads were counted and used for mapping to the circRNA junction with an overhang of  $\geq 6$  nt for each candidate.

### Cell culture and transfection

Human glioma cell lines LN229, SHG44, U251, and T98G along with normal glial HEB cell lines were purchased from the Chinese Academy of Sciences Cell Bank (Shanghai, China). We cultured HEB cells in RPMI-1640 medium and cultured Glioma cell lines in DMEM medium supplied with 10% FBS and 1% Penicillin-Streptomycin Solution (Gibco, USA). The cells were maintained in an incubator at 37°C with 5% CO<sub>2</sub>.

SATB1 overexpression vector was constructed by inserting SATB1 cDNA into the pcDNA3.1 vector. Then, *miR-590-5p* mimics and hsa\_circ\_0010889 siRNA were synthesized by Genepharma (Suzhou, China). Cell transfection was performed at 70% confluency according to Lipofectamine 2000 manufacturer's instructions. After two days, the cells were harvested for downstream experiments.

### Fluorescence *in situ* hybridization (FISH)

Specific probes for hsa\_circ\_0010889 (Dig-5'-CTTGC CAGACTTAAGCTTTTTACGACGCG-3'-Dig) were

synthesized (Geneseed Biotech, Guangzhou, China) and signals were captured via Cy3-conjugated anti-biotin antibodies (GenePharma, Shanghai, China). 4,6-diamidino-2-phenylindole (DAPI) was also utilized to counterstain for cell nuclei. Finally, we imaged the cells using a Zeiss LSM 700 confocal microscope (Carl Zeiss, Oberkochen, Germany).

### Western blot assay

Protein samples were extracted from cells with RIPA lysis buffer for western blot assays. Anti-E-cadherin (1:1,000), anti-N-cadherin (1:1,000), and anti-GAPDH (1:1,000) primary antibodies were obtained from Cell Signaling Technology (Beverly, MA, USA) and used to stain protein blots following the manufacturer's instructions. Immunoreactivity was visualized using a chemiluminescence detection kit (ECL; Western Blotting Substrate, Donghuan Biotech, Dongguan, China).

### Quantitative real-time polymerase chain reaction (RT-qPCR)

Total cellular RNA was extracted using a TRIzol reagent kit (Invitrogen, Carlsbad, CA, USA) and cDNA was synthesized for subsequent qPCR using a TaqMan Assay Kit (Applied Biosystems, Foster City, CA, USA) and the  $2^{-\Delta\Delta CT}$  approach was used to obtain relative expression fold changes. *U6* and *GAPDH* were employed as internal references. The following primers were used: hsa\_circ\_0010889 primers forward, 5'-CCTAATAAATCCTTGC-3' and reverse, 5'-CAGC TCCGGCAACTAAGCGCGC-3'. *miR-590-5p* primers forward, 5'-GAGCTTATTCATAAAAAGT-3'; and reverse: 5'-TCCACGACACGCACTGGATACGAC-3'. *U6* primers were forward, 5'-CTCGCTTCGGCAGC ACA-3'; and reverse: 5'-AACGCTTCACGAATTTG CGT-3'; *GAPDH* primers were forward, 5'-AATGGG CAGCCGTTAGGAAA-3'; and reverse: 5'-TGAAGGG GTCATTGATGGCA-3'.

### 5-Ethynyl-2'-deoxyuridine (EdU) assay

DNA synthesis and cell proliferation were analyzed using an EdU assay kit (RiboBio, Guangzhou, China). Here,  $1 \times 10^4$  of LN229 and U251 cells were seeded into 96-well plates overnight. On the second day, EdU solution (25  $\mu$ M) was added to the wells and incubated for 24 h. Then, 4% formalin was utilized to fix the cells for 2 h at room temperature. We utilized Triton X-100 to permeabilize the cells for ten minutes, and then added 200  $\mu$ L Apollo reaction solution to stain EdU and 200  $\mu$ L of DAPI solution to stain cell nuclei for 0.5 h. DNA synthesis and cell proliferation were measured using a fluorescence microscope (Nikon, Tokyo, Japan).

## Cell proliferation assay

We seeded  $2 \times 10^3$  cells into 96-well plates and the absorbance at 450 nm was read for every sample using the CCK-8 assay (Yeasen Biotech Co., Ltd., Shanghai, China). Finally, we constructed a cell viability curve.

## Transwell migration assay

Transfected cells after 48 h were diluted  $2.0 \times 10^5$ /mL and briefly, 200  $\mu$ L/well of cell suspension was added to the Transwell chamber (Millipore, Billerica, MA, USA) upper side. At the same time, we added 500  $\mu$ L of medium containing 10% FBS to the lower chamber. After a 24 h incubation, we fixed the cells that had migrated to the bottom side with paraformaldehyde for 15 min, and then stained them with crystal violet for 5 mins. Cells were observed under a microscope and the migration cell numbers were counted. We randomly selected and counted five fields of view for every sample.

## Dual-luciferase reporter assay

Putative miR-590-5p binding site in the 3'-UTR for the target gene SATB1 and hsa\_circ\_0010889 (Mut/WT) were cloned into the psi-CHECK (Promega, Madison, WI, USA) vector downstream of firefly luciferase 3'-UTR or hsa\_circ\_0010889. The primary luciferase signal was normalized to Renilla luciferase as the normalization signal. The relative Renilla luciferase activity was analyzed according to the provided protocols (Promega, Mannheim, Germany).

## *In vivo* experiments

To establish the nude mouse model for glioma, LN229 cells ( $1 \times 10^6$ ) with sh-NC or sh-hsa\_circ\_0010889 were injected into the flank of nude mice. We then measured tumor volume and weight.

For tumor metastasis experiments, luminescence-labeled LN229 cells transfected with sh-NC or sh-hsa\_circ\_0010889 ( $1 \times 10^5$ ) were injected into each nude mouse tail vein and post 4 weeks, lung metastasis was assessed using an *in vivo* bioluminescence imaging system and computed metastatic foci counts in lung tissues post H&E staining.

## Statistical analysis

Data were represented as means  $\pm$  standard deviation (SD) and statistical analyses were performed using GraphPad Prism (La Jolla, CA, USA) to determine statistical significance between groups. A *P*-value of  $\leq 0.05$  was considered to be statistically significant.

A two-tailed Student's *t*-test was used to determine significant differences between two groups, and one-way ANOVA with post hoc Bonferroni test was applied to identify significant differences among three or more groups.

## Availability of data and materials

The datasets used and/or analyzed during the present study are available from the corresponding author on reasonable request.

## RESULTS

### A key role for hsa\_circ\_0010889 in glioma progression

Accumulating evidence suggests that circRNA has an important function in glioma progression [8, 9]. However, its regulatory mechanism is unknown. In our current investigation, we employed next-generation sequencing (NGS) and found that circRNA displayed abnormal expression in glioma tissues when compared to adjacent normal tissues (Figure 1A). Furthermore, RT-qPCR showed high levels of circRNA hsa\_circ\_0010889 expressions as detected by NGS. Our data show that hsa\_circ\_0010889 expression was significantly upregulated in glioma tissues (Figure 1B) and RT-qPCR showed that circ-PITHD1 expression increased in several glioma cell lines (SHG44, U251, T98G and LN229) when compared to normal glial HEB cell lines. U251 and LN229 cells have higher hsa\_circ\_0010889 expression (Figure 1C). FISH data showed that hsa\_circ\_0010889 expression increased in glioma tumor tissues when compared to adjacent normal tissues (Figure 1D).

### hsa\_circ\_0010889 downregulation suppressed glioma growth and proliferation *in vivo* and *in vitro*

To determine a role for hsa\_circ\_0010889 in glioma progression, we constructed an siRNA against hsa\_circ\_0010889 (si-hsa\_circ\_0010889), and transfected this into both LN229 and U251 cells. Results showed that hsa\_circ\_0010889 significantly decreased post hsa\_circ\_0010889 silencing in U251 and LN229 cells (Figure 2A). Our CCK8 (Figure 2B, 2C) and EdU (Figure 2D, 2E) assays showed that downregulation of hsa\_circ\_0010889 significantly decreased the proliferation ability of both LN229 and U251 cells. The tumor progression in xenografted nude mice using LN229 cells showed that silencing hsa\_circ\_0010889 significantly decreased tumor growth in both weight and volume (Figure 2F–2H). Immunohistochemical staining for Ki67 confirmed that hsa\_circ\_0010889 silencing inhibited Ki67 expression in tumor tissues (Figure 2I, 2J) implying that

hsa\_circ\_0010889 downregulation inhibited glioma proliferation and tumor growth *in vitro* and *in vivo* experiments.

**hsa\_circ\_0010889 downregulation inhibited glioma pulmonary metastasis and migration *in vitro* and *in vivo***

Transwell assays looking at migration showed that hsa\_circ\_0010889 silencing inhibited migration in both LN229 and U251 cells (Figure 3A, 3B) and live imaging data revealed that LN229 cells metastasized to the pulmonary system and that hsa\_circ\_0010889 silencing decreases this pulmonary metastatic capability. H&E staining also confirmed that hsa\_circ\_0010889 silencing reduced metastatic foci count in lung tissues (Figure 3C–3E) suggesting that hsa\_circ\_0010889 downregulation inhibited glioma cells invasion.

**SATB1 and miR-590-5p are downstream targets for hsa\_circ\_0010889**

Bioinformatics results found that hsa\_circ\_0010889 interacted with miR-590-5p. A luciferase reporter analysis further confirmed that miR-590-5p inhibited luciferase function in WT cells (Figure 4A, 4B), suggesting that miR-590-5p was the downstream target of hsa\_circ\_0010889.

Bioinformatics data also found that SATB1 was the miR-590-5p downstream target. Therefore, to better validate the association between SATB1 and miR-590-5p, WT/MUT 3'UTR-SATB1 sequences including a miR-590-5p binding sequence were constructed into a luciferase reporter vector (Figure 4C), which we transfected into LN229 cells integrated in the presence or absence of a miR-590-5p mimic. Luciferase reporter results confirmed that miR-590-5p suppressed luciferase

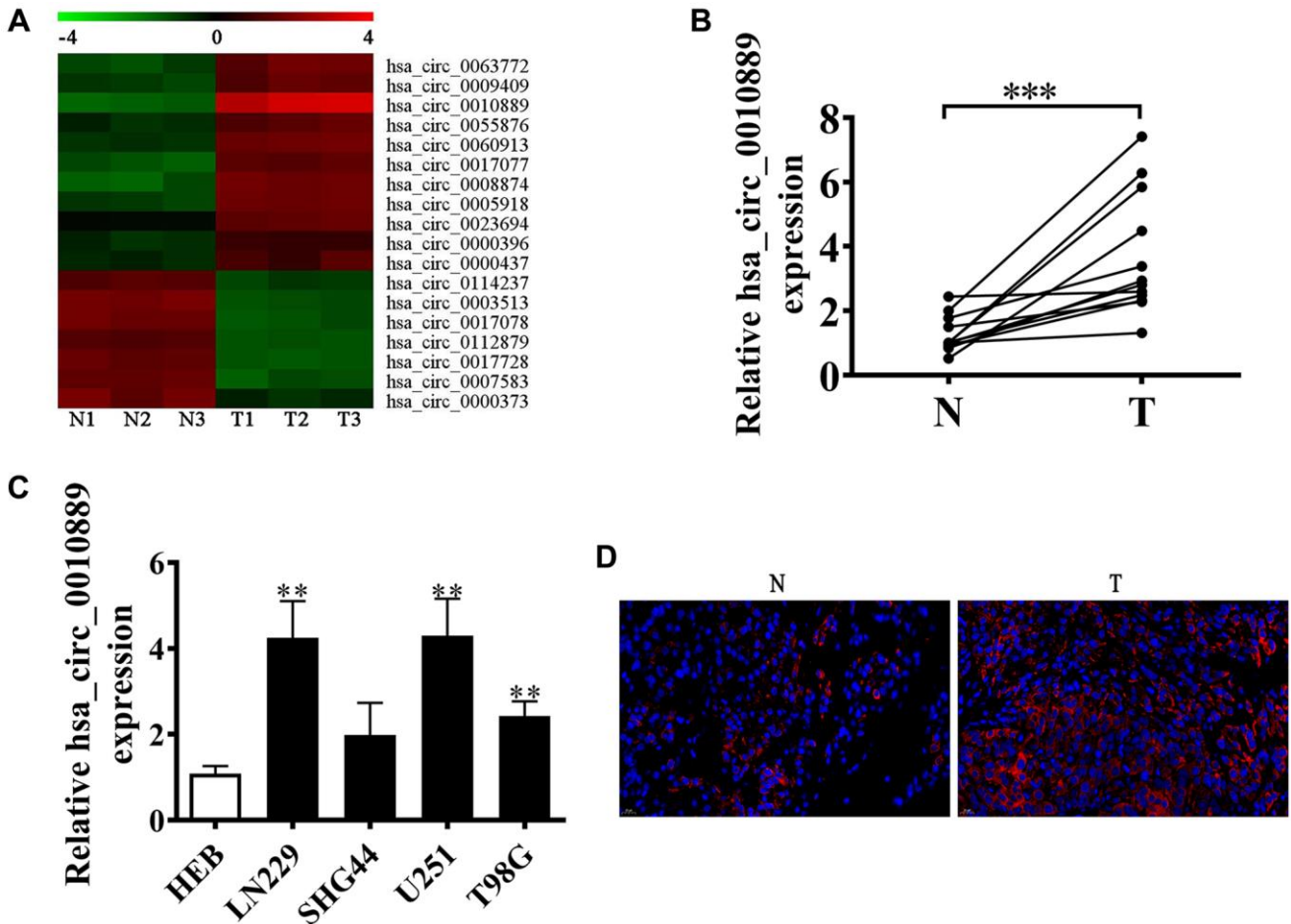


**Figure 1. hsa\_circ\_0010889 plays a key role in the progression of glioma. (A)** Heat map showing the expression of circRNA in CRC tumor tissues and adjacent normal tissues. **(B)** RT-qPCR detection shows the expression of five highly expressed circRNAs in glioma tumor tissues and adjacent normal tissues. The data are presented as the mean ± SD. \*\*\**p* < 0.001 vs. Normal. **(C)** RT-qPCR detection showing the expression of hsa\_circ\_0010889 in the glioma cell lines LN229, SHG44, U251, and T98G and the normal glioma cell line HEB. The data are presented as the mean ± SD. \*\**p* < 0.01 vs. HEB. **(D)** FISH detection showing the expression and subcellular distribution of hsa\_circ\_0010889.

function in WT cells (Figure 4D), showing that SATB1 was the downstream target for miR-590-5p.

Furthermore, RT-qPCR results showed that hsa\_circ\_0010889 expression decreased post transfected with hsa\_circ\_0010889 silencing vector. But a miR-590-5p inhibitor or overexpression of SATB1 had no effect on hsa\_circ\_0010889 expression in U251 and LN229 cells (Figure 4E, 4F), suggesting that SATB1 and miR-590-5p were downstream targets of hsa\_circ\_0010889. RT-qPCR data also found that hsa\_circ\_0010889 silencing increased miR-590-5p

expression and that SATB1 overexpression had no effect on si-hsa\_circ\_0010889-induced miR-590-5p expression inhibition (Figure 4G, 4H), suggesting that miR-590-5p was downstream of hsa\_circ\_0010889. Results also showed that hsa\_circ\_0010889 silencing decreased SATB1 expression. However, miR-590-5p downregulation reversed the inhibitory effects of si-hsa\_circ\_0010889 to SATB1 expression. When using the post SATB1 overexpression vector, we found that SATB1 expression increased significantly (Figure 4I, 4J) implying that hsa\_circ\_0010889 promoted SATB1 expression via sponging of miR-590-5p.

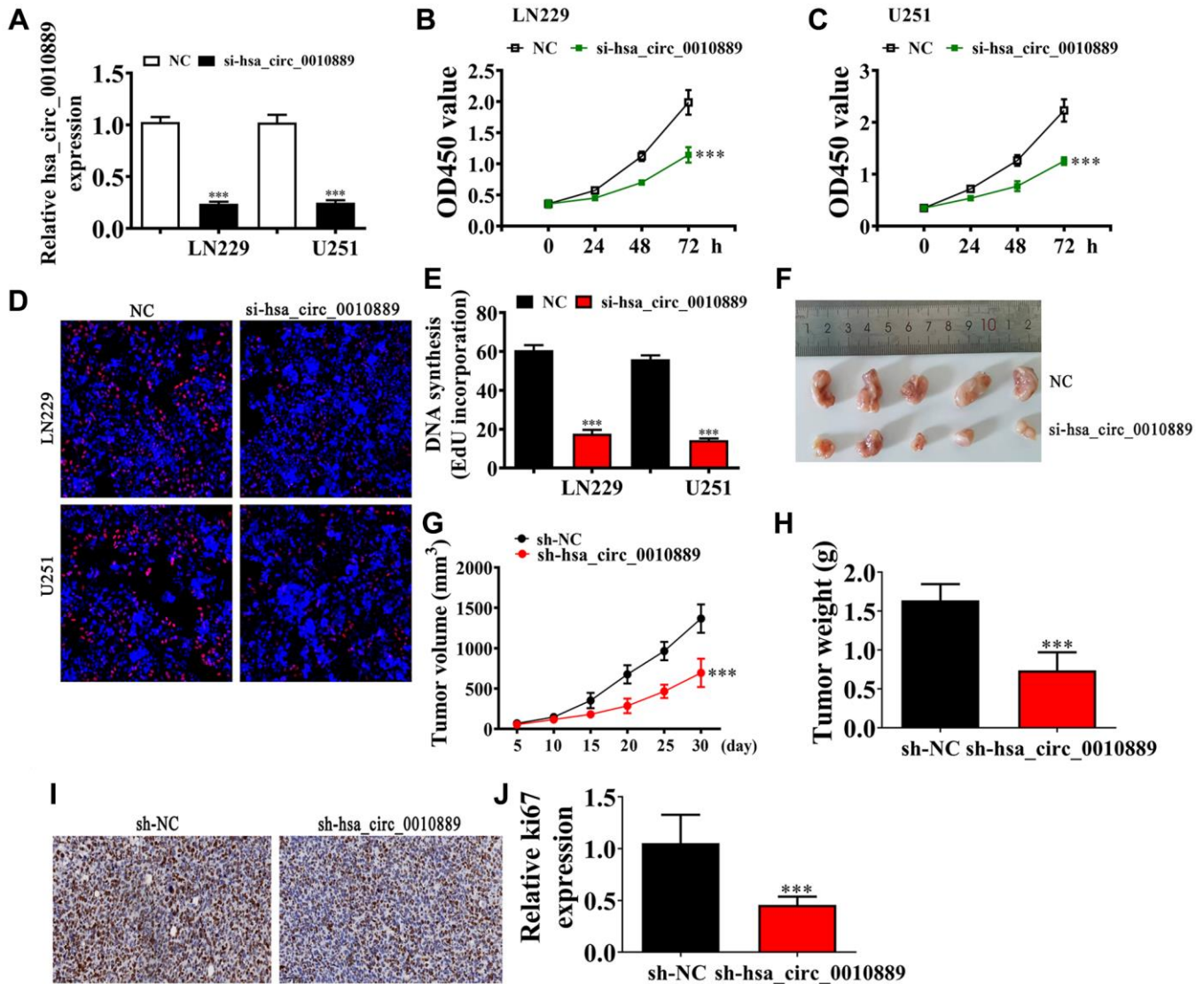


**Figure 2. Downregulation of hsa\_circ\_0010889 suppressed glioma proliferation and tumor growth both *in vivo* and *in vitro*.** (A) RT-qPCR detection showing the expression of hsa\_circ\_0010889 in both LN229 and U251 cells. The data are presented as the mean  $\pm$  SD. \*\*\* $p$  < 0.001 vs. NC. (B, C) CCK8 detection showing the effect of hsa\_circ\_0010889 on glioma cell proliferation. The data are presented as the mean  $\pm$  SD. \*\*\* $p$  < 0.001 vs. NC. (D, E) EdU detection showing cell proliferation in both LN229 and U251 cells. Data are presented as the mean  $\pm$  SD. \*\*\* $P$  < 0.001 vs. sh-NC. (F) Representative images of LN229 tumor formation in xenografts from nude mice. (G, H) Summary of tumor volumes and weights in mice. Data are presented as the mean  $\pm$  SD. \*\*\* $P$  < 0.001 vs. sh-NC. (I, J) Immunohistochemical staining showing the percentage of Ki-67-positive cells and relative Ki-67-positive cells were calculated. Data are presented as the mean  $\pm$  SD. \*\*\* $P$  < 0.001 vs. sh-NC.

**SATB1 overexpression or miR-590-5p inhibition restored glioma cell proliferation and migration post silencing of hsa\_circ\_0010889**

Using EdU (Figure 5A–5D) we found that SATB1 overexpression or miR-590-5p inhibition restored

glioma cell proliferation ability in both LN229 and U251 cells post hsa\_circ\_0010889 silencing (Figure 5C–5E). Transwell assays for the detection of migration showed that SATB1 overexpression or miR-590-5p suppression restored glioma cell migration ability in LN229 and U251 cells post silencing of

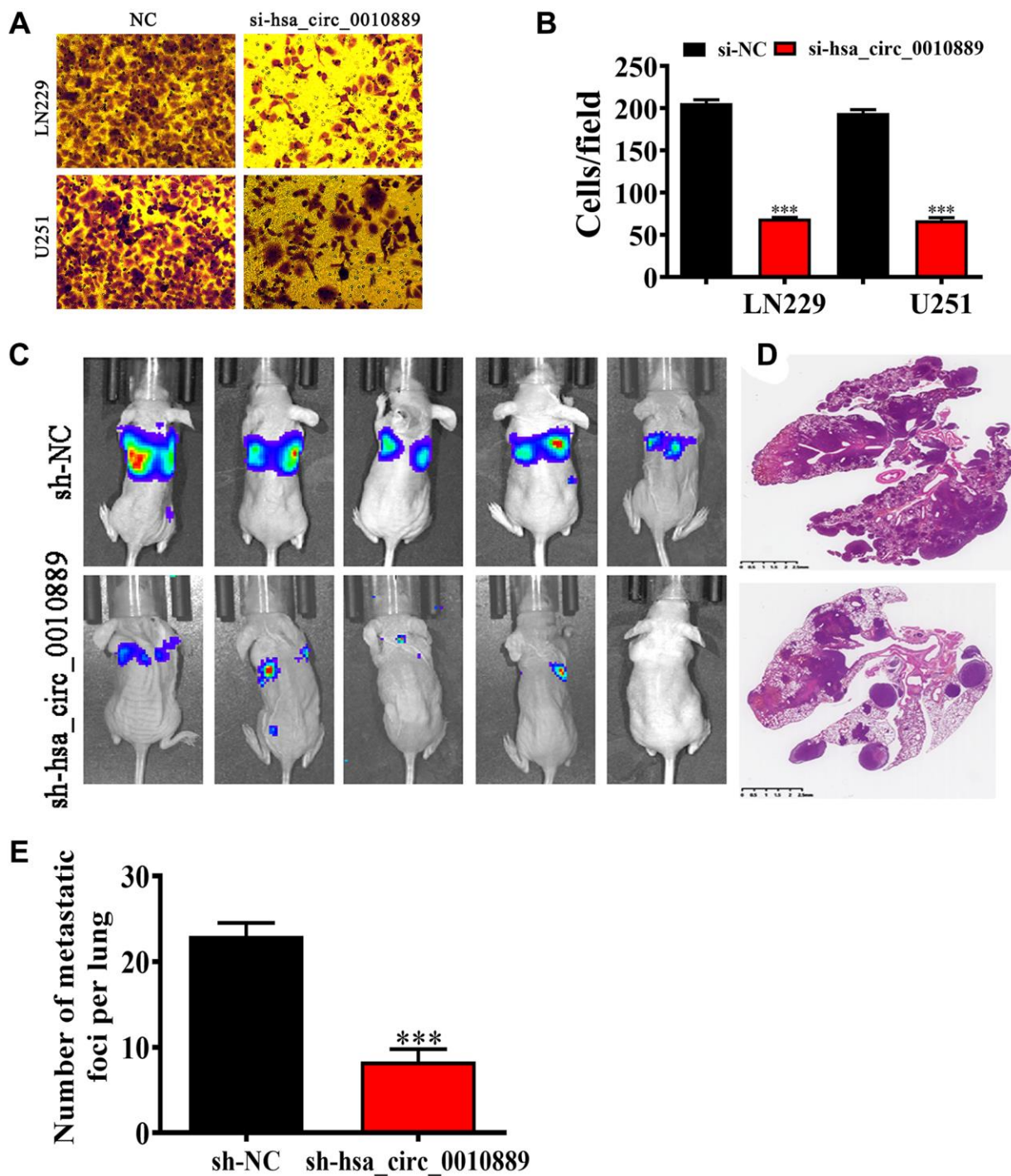


**Figure 3. Downregulation of hsa\_circ\_0010889 suppressed glioma migration and pulmonary metastasis both *in vivo* and *in vitro*.** (A, B) Transwell detection showing the migration of both LN229 and U251 cells after transfection with si-hsa\_circ\_0010889. Data are presented as the mean  $\pm$  SD. \*\*\* $P < 0.001$  vs. si-NC. (C) Live image detection showing LN229 cell pulmonary metastasis. (D, E) The numbers of metastatic foci in lung tissues were calculated according to the H&E staining. The data are expressed as the mean  $\pm$  SD. \*\*\* $p < 0.001$  vs. sh-NC.

hsa\_circ\_0010889 (Figure 5E–5H). Western blot detection show that SATB1 overexpression or miR-590-5p inhibition restored glioma cell EMT-related protein expression post silencing of hsa\_circ\_0010889 (Figure 5I and 5J).

### Overexpression of SATB1 restored glioma cell proliferation and migration after miR-590-5p overexpression

Again, using EdU (Figure 6A–6D) detection we found that overexpression of SATB1 restored glioma cell proliferation in both LN229 and U251 cells post miR-590-5p overexpression (Figure 5C–5E). Transwell assays also showed that overexpression of SATB1 restored glioma cell migration ability in both U251 and LN229 cells after overexpression of miR-590-5p (Figure 6E–6H). Western blot results showed that SATB1 overexpression restored EMT-related protein expression after miR-590-5p overexpression (Figure 6I and 6J).

## DISCUSSION

Accumulating studies have found that circRNAs are partially responsible for tumorigenesis and glioma progression [10]. Our present investigation found increased hsa\_circ\_0010889 expression in glioma tissues and cell lines suggesting that hsa\_circ\_0010889 is important during glioma progression. Furthermore, hsa\_circ\_0010889 downregulation inhibited glioma proliferation and invasion but the regulatory mechanisms remain to be elucidated.

Bioinformatics data found that SATB1 and miR-590-5p were downstream targets for hsa\_circ\_0010889 and this was confirmed by luciferase reporter assay. hsa\_circ\_0010889 downregulation promoted miR-590-5p expression and importantly previous investigations found that circ\_0069718 promotes breast cancer via upregulation of NFIB and targets miR-590-5p directly [11]. miR-590-5p has been found to suppress malignant melanoma cell growth and invasions by targeting Skp2 [12] and downregulation of circ-PITHD1 can inhibit colorectal cancer through suppression and the miR-590-5p/HK2 axis [13]. Our present investigation discovered that miR-590-5p overexpression reversed the inhibitory effects of si-hsa\_circ\_0010889 on glioma proliferation and migration suggesting that hsa\_circ\_0010889 silencing can inhibit glioma progression by the promotion of miR-590-5p expression.

Further investigations have found that SATB1 is a downstream target for miR-590-5p which was confirmed by luciferase reporter assay. hsa\_circ\_0010889 downregulation inhibits SATB1 expression but inhibition of miR-590-5p reversed this inhibitory effect with respect to si-hsa\_circ\_0010889 and SATB1 expression. Previous studies have found that SATB1 has an important function to regulate invasion and metastasis in breast cancer [14]. Furthermore, SATB1 is highly expressed in several cancer cell types [15]. SATB1 has been shown to influence the epithelial-mesenchymal transition (EMT) in lung cancer [16]. The present study also found that hsa\_circ\_0010889 silencing inhibited EMT-related protein N-cadherin expression and promoted E-cadherin

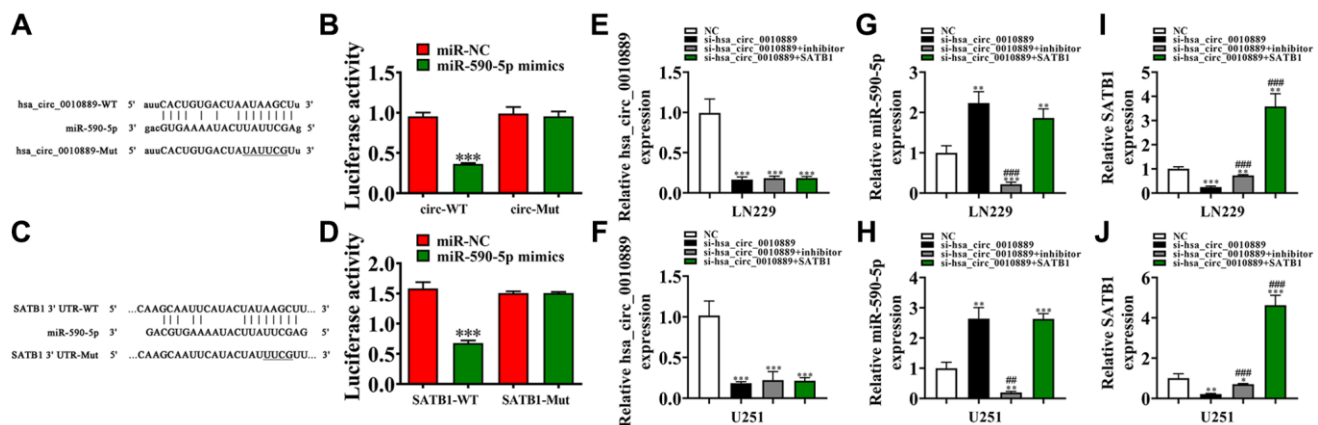


**Figure 4. Both miR-590-5p and SATB1 were the downstream targets for hsa\_circ\_0010889.** (A) Prediction of binding sites of miR-590-5p in hsa\_circ\_0010889. The MUT version of hsa\_circ\_0010889 is presented. (B) Relative luciferase activity determined 48 h after transfection of LN229 cells with miR-590-5p mimic/NC or hsa\_circ\_0010889 WT/Mut. Data are presented as means  $\pm$  SD. \*\*\* $P$  < 0.001. (C) Prediction of binding sites of miR-590-5p within the 3'UTR of SATB1. The MUT version of the 3'-UTR-SATB1 is shown. (D) Relative luciferase activity determined 48 h after transfection of LN229 cells with miR-590-5p mimic/NC or 3'UTR-SATB1 WT/Mut. Data are presented as means  $\pm$  SD. \*\*\* $P$  < 0.001. (E–J) RT-qPCR detection showing the expression of hsa\_circ\_0010889, miR-590-5p and SATB1 in both LN229 and U251 after transfection with si-hsa\_circ\_0010889, miR-590-5p inhibitor and SATB1 overexpression vector together or single. Data are presented as means  $\pm$  SD. \* $P$  < 0.05, \*\* $P$  < 0.01, \*\*\* $P$  < 0.001 vs. NC. ## $P$  < 0.01, ### $P$  < 0.001 vs. si-hsa\_circ\_0010889.

expression. SATB1 overexpression restored EMT-related protein N-cadherin expression and promoted E-cadherin expression. In addition, hsa\_circ\_0010889 silencing inhibited SATB1 expression, while SATB1 overexpression restored SATB1 levels. SATB1 over-

expression also restored migratory ability post hsa\_circ\_0010889 silencing, suggesting that removing the effect of hsa\_circ\_0010889 can inhibit glioma progression by promotion miR-590-5p and inhibiting SATB1 expression.

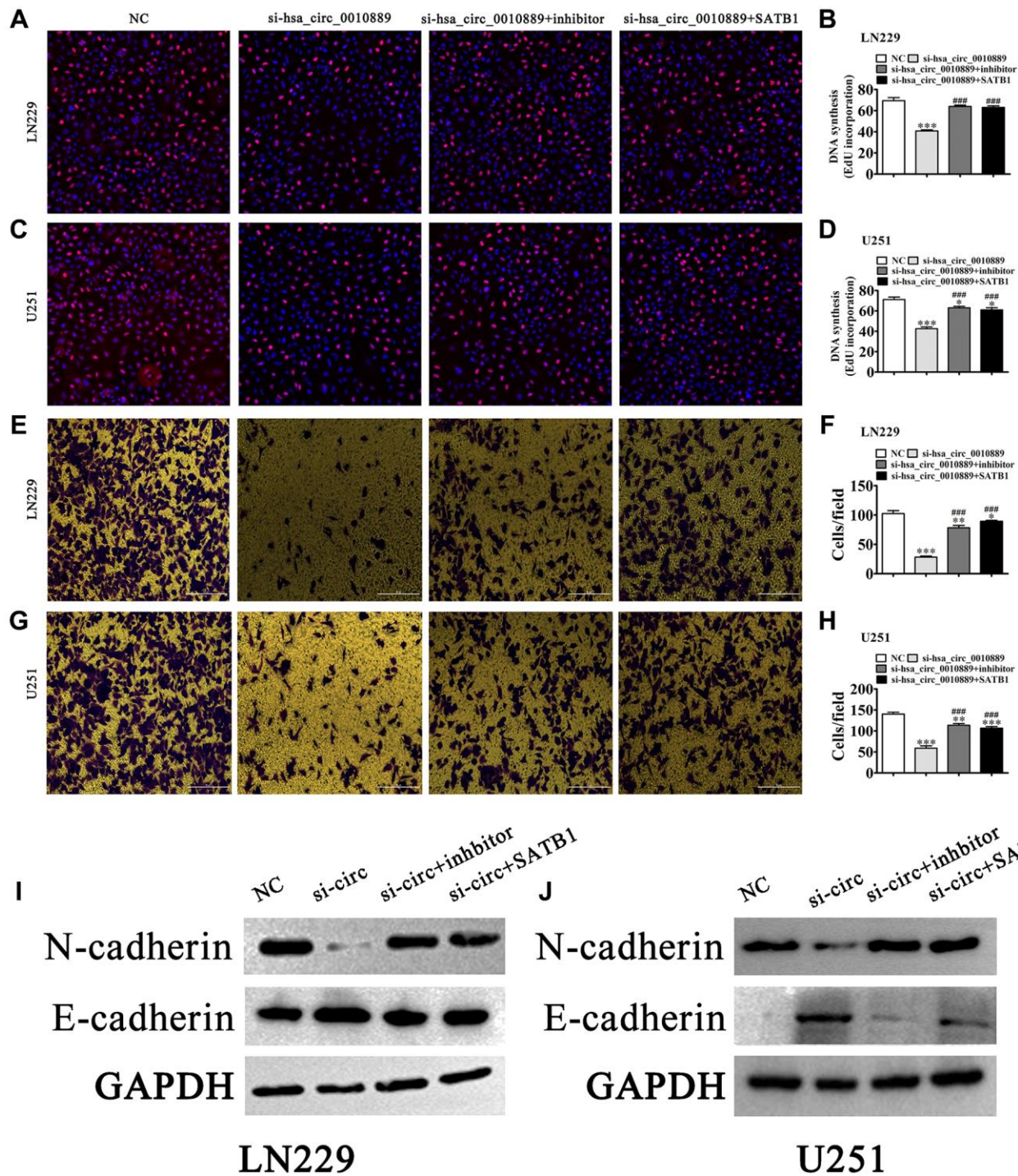


**Figure 5. Overexpression of SATB1 or inhibition of miR-590-5p reversed glioma cell proliferation and migration after silencing hsa\_circ\_0010889.** (A–D) EdU detection showing the proliferative ability of LN229 and U251 cells. The data are expressed as the mean  $\pm$  SD. \* $P < 0.05$ , \*\*\* $P < 0.001$  vs. NC. ### $P < 0.001$  vs. si-hsa\_circ\_0010889. (E–H) Transwell detection showing migration of LN229 and U251 cells. The data are expressed as the mean  $\pm$  SD. \* $P < 0.05$ , \*\* $P < 0.01$ , \*\*\* $P < 0.001$  vs. NC. ### $P < 0.001$  vs. si-hsa\_circ\_0010889. (I, J) Western blot results showing the expression of E-cadherin and N-cadherin.

Our investigation provides evidence that hsa\_circ\_0010889 downregulation can reduce glioma proliferation and invasion via miR-590-5p/SATB1 signaling mediated by the regulation of aerobic

glycolysis. Our data has revealed that hsa\_circ\_0010889 is a promising marker for glioma diagnostics, and which may be extended to the development of drugs targeting hsa\_circ\_0010889, for the treatment of glioma.

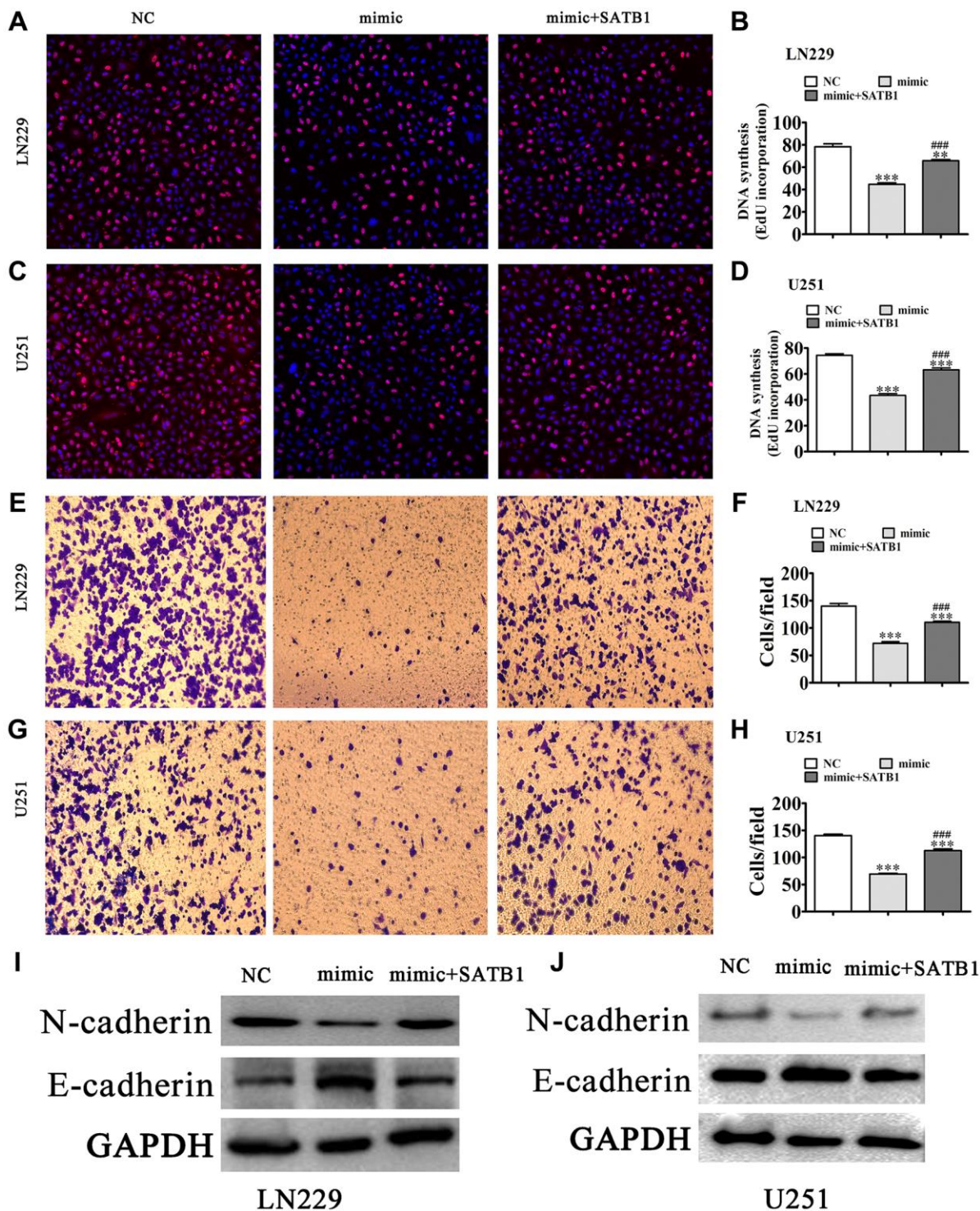


**Figure 6. Overexpression of SATB1 reversed glioma cell proliferation and migration after overexpression of miR-590-5p.** (A–D) EdU detection showing the proliferative ability of LN229 and U251 cells. The data are expressed as the mean  $\pm$  SD.  $**P < 0.01$ ,  $***P < 0.001$  vs. NC.  $###P < 0.001$  vs. mimic. (E–H) Transwell detection showing invasion and migration of LN229 and U251 cells. The data are expressed as the mean  $\pm$  SD.  $***P < 0.001$  vs. NC.  $###P < 0.001$  vs. si-hsa\_circ\_0010889. (I, J) Western blot results showing the expression of E-cadherin and N-cadherin.

## AUTHOR CONTRIBUTIONS

Z.W. and Q.L.G. contributed to the study conception and design. All authors collected the data and performed the data analysis. Z.W. and Q.L.G. performed experiments and analyzed and interpreted the data. All authors contributed to the drafting of the article and final approval of the submitted version.

## CONFLICTS OF INTEREST

The authors declare no conflicts of interest related to this study.

## ETHICAL STATEMENT

This study was approved by the Ethics Committee of The First Hospital of Lanzhou University (LDYYLL2021-23). All applicable international, national, and/or institutional guidelines for the care and use of animals were followed.

## FUNDING

The study was supported by the Natural Science Foundation of Gansu Province (No. 20JR10RA687), Health industry research Project of Gansu Province (No. GSWSKY2021-004), and Hospital Fund of Lanzhou University First Hospital (No. Idyyyn2019-51).

## REFERENCES

1. Lapointe S, Perry A, Butowski NA. Primary brain tumours in adults. *Lancet*. 2018; 392:432–46. [https://doi.org/10.1016/S0140-6736\(18\)30990-5](https://doi.org/10.1016/S0140-6736(18)30990-5) PMID:30060998
2. Yang K, Wu Z, Zhang H, Zhang N, Wu W, Wang Z, Dai Z, Zhang X, Zhang L, Peng Y, Ye W, Zeng W, Liu Z, Cheng Q. Glioma targeted therapy: insight into future of molecular approaches. *Mol Cancer*. 2022; 21:39. <https://doi.org/10.1186/s12943-022-01513-z> PMID:35135556
3. Glaser T, Han I, Wu L, Zeng X. Targeted Nanotechnology in Glioblastoma Multiforme. *Front Pharmacol*. 2017; 8:166. <https://doi.org/10.3389/fphar.2017.00166> PMID:28408882
4. Parsons DW, Jones S, Zhang X, Lin JC, Leary RJ, Angenendt P, Mankoo P, Carter H, Siu IM, Gallia GL, Olivi A, McLendon R, Rasheed BA, et al. An integrated genomic analysis of human glioblastoma multiforme. *Science*. 2008; 321:1807–12. <https://doi.org/10.1126/science.1164382> PMID:18772396
5. Pan Z, Zhao R, Li B, Qi Y, Qiu W, Guo Q, Zhang S, Zhao S, Xu H, Li M, Gao Z, Fan Y, Xu J, et al. EWSR1-induced circNEIL3 promotes glioma progression and exosome-mediated macrophage immunosuppressive polarization via stabilizing IGF2BP3. *Mol Cancer*. 2022; 21:16. <https://doi.org/10.1186/s12943-021-01485-6> PMID:35031058
6. Xia H, Liu B, Shen N, Xue J, Chen S, Guo H, Zhou X. circRNA-0002109 promotes glioma malignant progression via modulating the miR-129-5P/EMP2 axis. *Mol Ther Nucleic Acids*. 2021; 27:1–15. <https://doi.org/10.1016/j.omtn.2021.11.011> PMID:34938603
7. Zhang S, Guan N, Mao X, Cui J, Sui X, Guo W. Exosomal circRNA\_104948 Enhances the Progression of Glioma by Regulating miR-29b-3p and DNMT3B/MTSS1 Signaling. *J Environ Pathol Toxicol Oncol*. 2022; 41:47–59. <https://doi.org/10.1615/JEnvironPatholToxicolOncol.2021039775> PMID:35695651
8. Meng X, Tian H, Guo W, Wang Z. circ\_0082375 promotes the progression of glioma by regulating Wnt7B. *Transl Neurosci*. 2021; 12:456–68. <https://doi.org/10.1515/tnsci-2020-0181> PMID:34868669
9. Wang P, Wang T, Dong L, Xu Z, Guo S, Chang C. Circular RNA circ\_0079593 facilitates glioma development via modulating miR-324-5p/XBP1 axis. *Metab Brain Dis*. 2022; 37:2389–403. <https://doi.org/10.1007/s11011-022-01040-2> PMID:35793013
10. Peng D, Luo L, Zhang X, Wei C, Zhang Z, Han L. CircRNA: An emerging star in the progression of glioma. *Biomed Pharmacother*. 2022; 151:113150. <https://doi.org/10.1016/j.biopha.2022.113150> PMID:35623170
11. Zhao Y, Ma X, Shi W. Circ\_0069718 promotes the progression of breast cancer by up-regulating NFIB through sequestering miR-590-5p. *Mamm Genome*. 2021; 32:517–29. <https://doi.org/10.1007/s00335-021-09923-y> PMID:34632534. Retraction in: *Mamm Genome*. 2023. [Epub ahead of print]. <https://doi.org/10.1007/s00335-023-10001-8> PMID:37306744
12. Tong Y, Jin L. miR-590-5p Targets Skp2 to Inhibit the Growth and Invasion of Malignant Melanoma Cells. *Dis Markers*. 2022; 2022:8723725. <https://doi.org/10.1155/2022/8723725>

PMID:[35845132](#)

13. Yang S, Zhao K, Yang X, Xing C. Downregulation of Circ-PITHD1 Suppressed Colorectal Cancer via Glycolysis Inhibition through miR-590-5p/HK2 Axis. *Evid Based Complement Alternat Med.* 2022; 2022:7696841.  
<https://doi.org/10.1155/2022/7696841>  
PMID:[36276867](#)
14. Chen Z, Sang MX, Geng CZ, Jia HQ. MicroRNA-409 regulates the proliferation and invasion of breast cancer cell lines by targeting special AT-rich sequence-binding protein 1 (SATB1). *Bioengineered.* 2022; 13:13045–54.  
<https://doi.org/10.1080/21655979.2022.2073320>  
PMID:[35611599](#)
15. Vickridge E, Faraco CCF, Nepveu A. Base excision repair accessory factors in senescence avoidance and resistance to treatments. *Cancer Drug Resist.* 2022; 5:703–20.  
<https://doi.org/10.20517/cdr.2022.36>  
PMID:[36176767](#)
16. Glatzel-Plucinska N, Piotrowska A, Rzechonek A, Podhorska-Okolow M, Dziegiel P. SATB1 protein is associated with the epithelial-mesenchymal transition process in non-small cell lung cancers. *Oncol Rep.* 2021; 45:118.  
<https://doi.org/10.3892/or.2021.8069>  
PMID:[33955522](#)